RECENT LANDSLIDES AND THEIR RELATION TO YOUNG THRUST FAULT SCARPS ON THE MOON. T. R. Watters[1], E. J. Speyerer, M. S. Robinson, [1]Center for Earth and Planetary Studies, National Air and Space Museum, Smithsonian Institution, Washington, DC 20560 USA, [2]Arizona State University, School of Earth and Space Exploration, Tempe, Arizona 85287, USA.

Introduction: One of the significant achievements of the Lunar Reconnaissance Orbiter (LRO) mission has been the detection of a global population of thousands of very young lobate thrust fault scarps [**1,2**]. Discovery of these small-scale contractional landforms continue with the acquisition of Lunar Reconnaissance Orbiter Camera (LROC) Narrow Angle Camera (NAC) images under optimum illumination geometries. The young age of the lobate fault scarps [**3–5**] raises the possibility that some may still be active [**2,6**]. Contemporary thrust faulting is consistent with modeling of the stress state of the Moon that indicates tidal forces are a significant component [**2,6,7**]. Tidal forces combined with isotropic compressional stresses resulting from global contraction due to the cooling of the lunar interior, influence the location and orientation of the thrust faults [**2,6,7**].

Slip events on active faults may have been recorded by the Apollo Seismic Network [**6**]. Four seismometers placed at the Apollo 12, 14, 15, and 16 landing sites operated from 1969 to 1977 and recorded 28 shallow moonquakes (SMQs) [**8,9,10**]. These SMQs registered Richter equivalent magnitudes ranging from 1.5 to ~5 and body wave magnitudes >5.5. Stress drops are estimated to be ≤10 MPa for 16 of the events and >10 MPa for 11 of the events [**11,12**]. To determine if the coseismic slip events on the faults were the source of some of the SMQs, the epicenter locations were relocated using an algorithm for sparse seismic networks. It was found that the epicenters of 13 of the SMQs fall within 90 km of a mapped thrust fault scarp [**6**]. A model of seismic shaking for a slip event on a typical lunar thrust fault suggests the distance of expected strong to moderate ground shaking is at least 60 km [**6**], and moderate to light shaking may extend beyond 90 km.

Seismic shaking from slip events on active thrust faults is expected to result in detectable changes to the lunar landscape. Landslides are likely to be the most common expression of changes induced by seismic activity, triggered on surfaces with significant topographic slopes. In addition to the slopes on fault scarp faces which can reach >10°, and those on highland massifs, the most common landforms with large slopes are the walls of impact craters and basins.

Landslides and Fault Scarps: LROC NAC temporal (before and after) image campaigns identified new impact craters and secondary impact process that formed during the LRO mission [**13**]. In the temporal image pairs collected between 2009 to 2015, 222 new impact craters were detected [**13**]. LROC temporal image campaigns are still ongoing. New craters and other surface changes are identified using an automated change-detection program (Change Recognition using Images with Similar Phase or CRISP) developed by the LROC team. Among the surface changes detected are landslides that occur on the walls of impact craters. A subset of the inventory of detected landslides can be directly attributed to new impacts or secondaries at or in close proximity to the head of the landslides. However, a number of the detected landslides cannot be spatially correlated with new impact craters or secondaries. To date, 24 such landslides have been identified in LROC temporal image pairs. The landsides are found on steeply sloping surfaces of crater walls at or near the angle of repose (mean slope ~34°), slopes expected to be particularly suspectable to landslides from seismic shaking. Using the center locations of lobate scarps in the current dataset (n > 3600), the preliminary analysis shows that 15 of the 24 landslides are within 90 km of a mapped fault scarp (Fig. 1, 2A). The 24 landslides have been detected in 19 craters, so multiple landslides have been found on the walls of five craters (Fig. 1). One of the craters, Briggs B (Fig. 1), has experienced four landslides over the 12-year period LRO has been acquiring images. Thus, the 15 landsides are within ~90 km of eight mapped fault scarps.

The spatial distribution of the 19 landslides within unique craters shows an apparent bias to the nearside mare (Fig. 1). However, 10 of the 19 craters with landslides are in the highlands. Many of the nearside craters with landslides are clustered near the tidal axis, where compressional stresses are predicted to reach a maximum.

Based on this analysis, we hypothesized that slip events on active thrust faults may have triggered some of the landslides. First, however, it is necessary to test the null hypothesis – i.e., whether the observed spatial correlation between the landslides and thrust faults is a random effect. To accomplish this, 1000 sets of 24 random landslide locations with slopes >15° have been generated. The proximity of the center location of each lobate scarp in the dataset is calculated for each random landslide in the sets and the number of random landslides within 90 km of a scarp is determined. The results show that none of the random sets have 15 landslides within 90 km of mapped scarps (Fig. 2B). Only five of the 1000 random sets (<1%) have as many as 11 random landslides within 90 km of a scarp. Thus, we conclude that landslides proximal to faults is not a random effect, and that some are being triggered by tectonic activity.

References: [1] Watters, T.R., et al. (2010) *Science*, *329*, 936-940, 10.1126/science.1189590. [2] Watters, T.R., et al. (2015) *Geology*, 43, 851–854. [3] Watters, T.R., et al. (2012) *Nature Geoscience*, *5*, 181–185, 10.1038/NGEO1387. [4] Clark, J.D., et al. (2017) *Icarus, 298*, 78-88. [5] van der Bogert, C. H., et al. (2018) *Icarus, 306*, 225-242. [6] Watters, T.R., et al. (2019) *Nature Geoscience, 12*, 411-417. [7] Matsuyama, I., et al. (2021) *Icarus*, *358*, doi.org/10.1016/j.icarus.2020.114202. [8] Nakamura, Y. (1980) *Proc. Lunar Planet. Sci. Conf. 11*, 1847-1853. [9] Nakamura, Y., et al. (1979) *Proc. Lunar Sci. Conf. 10th,* 2299-2309. [10] Nakamura, Y., et al. (1982) *J. Geophys. Res., 87*, A117-A123. [11] Binder, A.B., Oberst, J. (1985) Earth Planet. Sci. Lett 74, 149–154. [12] Oberst, J. (1987) *J. Geophys. Res., 92*, 1397–1405.[13] Speyerer, E.J. et al. (2016) *Nature,* 538, 215-218.

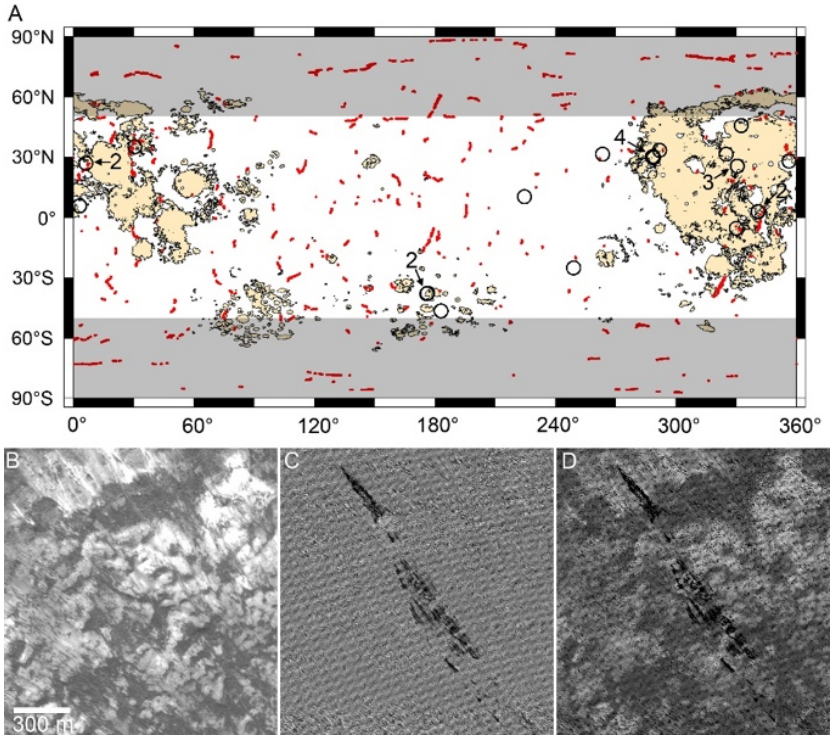

Figure 1. A) Locations of landslides (open black circles) detected in temporal images not connected with new impact events. Fifteen mapped lobate thrust fault scarps (red lines) are within 90 km of a recent landslide. Numbers indicate multiple landslides in a crater. Shading shows areas outside the optimum detection latitudes. B) LROC NAC temporal image before landslide (M1134365669L acquired on 2013-09-21). C) The ratio of temporal images (M1134365669L and M1164980196L acquired on 2014-09-10). D) The ratio image combined with the before landslide temporal image.

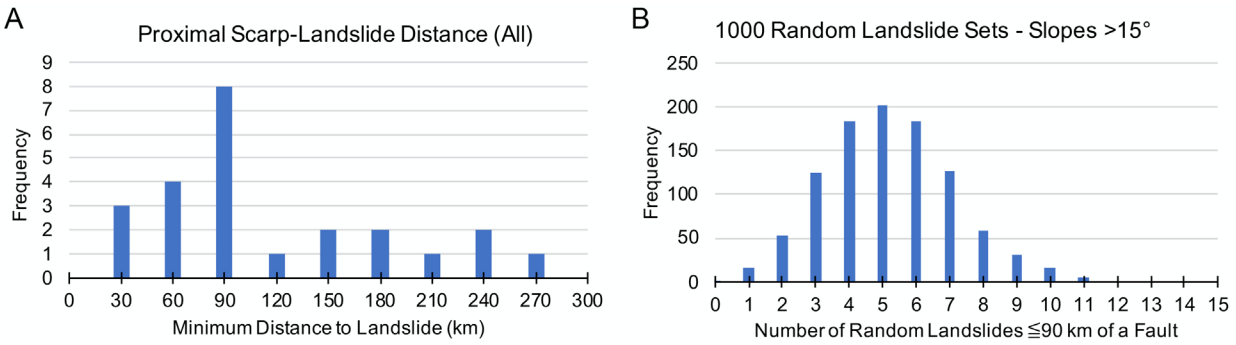

Figure 2. Histograms of the distribution of the distances between landslides and lobate scarps. A) Distribution of minimum distances between 24 landslide locations and mapped fault scarps. B) Distribution of minimum distance of 24,000 randomly generated landslide locations (in 1000 sets of 24) on slopes greater than 15° within 90 km of mapped fault scarps.